Journal of Magnetic Resonance **157,** 298–303 (2002)
doi:10.1006/jmre.2002.2595

COMMUNICATIONS

A Study of the Use of Overhauser Enhancement to Assist with Needle and Catheter Placement during Interventional MRI

Erkki Vahala,*[,1] Mika Ylihautala,† Gösta Ehnholm,* Nina Etelä,* Ian Young,† Klaes Golman,‡ and Ib Leunbach‡

*Philips Medical Systems MR Technologies Finland, Ltd., Vantaa, Finland; †Robert Steiner MRI Unit, Hammersmith Hospital, London, United Kingdom; and ‡Amersham Health AB

Received February 15, 2002; revised May 29, 2002

The practicability of using Overhauser enhancement of saline in interventional MRI was investigated. Saline was used as a means of marking the path taken by a fluid-filled cavity, similar to that formed by a needle, catheter, or cannula during interventional MRI procedures. A prototype device was designed and constructed for saturation and propulsion of 0.6 ml of doped liquid. The pertinent Overhauser parameters, such as the obtainable enhancement factor, were measured. Signal enhancement in excess of 10 was demonstrated in practice by acquiring images showing an enhancement of fluid in a catheter tube. © 2002 Elsevier Science (USA)

Key Words: **Overhauser enhancement; microwave polarization; electron spin resonance (ESR); interventional magnetic resonance imaging (IMRI); catheter placement.**

INTRODUCTION

A number of strategies have been considered as possible means of locating the position of a needle-like structure and any injection using them as part of the technical environment needed to support interventional MRI. In active tracking systems, the structure are localized with active elements *in vivo* (*1*), whereas in passive tracking, the methods have focused on the problem of controlling susceptibility artifacts of the structures (*2, 3*), with variants in which the artifact is modified to improve catheter visibility (*4, 5*) or achieve other desired effects. We have investigated an alternative passive tracking strategy in which the location of a needle is outlined by the signal from fluid flowing through and around it, similarly to contrast agent flooded structures (*6–8*), and provide the preliminary results on the technical aspects on what we believe is a novel method of highlighting the fluid.

In order to distinguish the fluid from the surrounding tissue, it is beneficial to enhance the signal from the fluid. We have done this using Overhauser enhancement from electron spins. Successful Overhauser enhancement results in a greatly enhanced signal that is clearly discernible from the signal of the surrounding tissue—a property that is useful at low-field strengths where the lack of signal strength is typically the limiting factor, especially for short sequences needed for instrument placement under MR guidance. The concept underlying approaches such as *p*roton-*e*lectron *d*ouble *r*esonance *i*maging (PEDRI) (*9*) or Overhauser marker enhancement (*10, 11*) assumes that the Overhauser enhancement is done *in vivo*. Due to safety concerns, irradiation power requirements, and high RF frequencies, this is technically very difficult in man, or animals. We avoid the difficulty by performing the enhancement prior to injection (describing this as *ex vivo*). This means that the irradiating structures can be substantially simpler and smaller. In addition, the risk associated with a patient being exposed to microwave heating is reduced.

The aim is to deliver the agent to the object of interest fast enough to retain most of the additional signal the Overhauser enhancement provides before proton spin-lattice relaxation eliminates it. Signal decay is particularly problematic with the trityl agents used in this work, as they are moderately efficient relaxation agents. The motion artifacts present during the fast injection determine the lower limit for the delay from the start of injection to the start of imaging.

THEORY OF DYNAMIC NUCLEAR POLARIZATION

Overhauser dynamic nuclear polarization (DNP) is a phenomenon in which the irradiation of an ensemble of electron spins, here denoted by S, at their characteristic Larmor frequency, results in transfer of electron spin polarization to the nuclear spin ensemble, denoted by I, provided that a suitable interaction exists between these two spin species. For a suitable paramagnetic substance, the steady-state ratio ε, which expresses the increase of the ensemble-averaged longitudinal nuclear magnetization of proton spins induced by irradiation of electron spins as compared to the equilibrium value of

[1] To whom correspondence should be addressed at Philips Medical Systems MR Technologies Finland, Inc., Ayritie 4, 01510, Vantaa, Finland. Fax: +358-9-25359 600. E-mail: Erkki.Vahala@philips.com.

1090-7807/02 $35.00

TABLE 1
Symbol List for Eq. [1]

Symbol	Description
I_z	Polarization of I-spins along the main magnetic field $\mathbf{B}_0$
I_0	Thermal equilibrium polarization of I-spins
S_z	Polarization of S-spins along $\mathbf{B}_0$
S_0	Thermal equilibrium polarization of S-spins
R_1^{II}	Cross-relaxation term for dipole–dipole-coupled unlike spins (affects time-differential dI_Z/dt through I_Z)
R_1^{IS}	Cross-relaxation term for dipole–dipole-coupled unlike spins (affects dI_Z/dt through S_Z)
R_{10}^{I}	Longitudinal relaxation rate of I-spins in the absence of S-spins
f	Leakage factor
A	Scaled coupling factor
s	Saturation factor

longitudinal proton magnetization, can be expressed by the basic DNP equation (*12*):

$$\varepsilon = \frac{I_Z - I_0}{I_0} = \frac{R_1^{II}}{R_1^{II} + R_{10}^{I}} \times \frac{S_0}{I_0}\,\frac{R_1^{IS}}{R_1^{II}} \times \frac{S_0 - S_Z}{S_0} = f \times A \times s. \quad [1]$$

See Table 1 for the detailed description of symbols. Above, the equation is expressed in a reduced form where the first term is nominated as a leakage factor f, the second a scaled coupling factor A, and the third a saturation factor s. These quantities have physically simple interpretations for a paramagnetic substance (*13*). The leakage factor describes the amount electrons are able to relax protons. Its maximum value of one would mean that electron-induced relaxation dominates proton relaxation over the other relaxation mechanisms, that is, $R_1^{II} \gg R_{10}^{I}$. The value of R_1^{II} depends on the amount of paramagnetic substance in solution. The dependency is found to be linear (see Ref. *13*), consequently R_1^{II} can be written as a product of concentration c and normalized relaxivity r:

$$R_1^{II} = rc \Rightarrow f = \frac{c}{c + R_{10}^{I}\, r^{-1}}. \quad [2]$$

Thus, for small c ($c \ll R_{10}^{I}\, r^{-1}$) the enhancement is linearly dependent on the concentration, but reaches an asymptotic limit as the concentration is increased. The scaled coupling factor includes a constant multiplier S_0/I_0, which helps to explain the choice of electrons as the second spin system. The gyromagnetic ratio and hence the equilibrium magnetization for electrons is approximately -658 times that of protons. The second term in A is the coupling factor $k = R_1^{IS}/R_1^{II}$. This introduces a dependency on the interaction mechanism affecting the two spin systems. For single electron agents in H_2O solutions, the dipolar coupling is dominant and, at sufficiently low magnetic fields fulfilling the extreme narrowing condition (*14*), k is equal to 0.5. The coupling value is reduced with increasing field strength.

The saturation factor depends on irradiation power and electron spin relaxation rates. Recent developments in ESR agents with closely spaced hyperfine lines have resulted in very narrow linewidths (*12*), thus enabling easy irradiation, which in turn means that the microwave power requirements for maximum enhancement are greatly diminished.

MATERIALS AND METHODS

Experiments were conducted at the proton resonance frequency of 9.8 MHz using a 0.23 T open-configuration magnet (Panorama 0.23 T, Philips Medical Systems, Best, The Netherlands).

The paramagnetic substance was a 5 mmol/l H_2O-based isotonic solution of an experimental trityl agent (Nycomed, Oslo, NC100135) with a typical ESR line width of 1 MHz in the oxygenated state and at room temperature. Compared with the more common nitroxide free radicals, trityl is easy to saturate, water soluble, biostable, and physiologically tolerable (*15*).

The basic properties of the trityl solution were measured, as a function of continuous-wave irradiation power and frequency, in a purpose-built glass container with a monopole antenna as a radiation source. Spin-lattice relaxation rates of protons for pure distilled water, i.e., R_{10}^{I}, and trityl solution, $R_1^{II} + R_{10}^{I}$, were determined with an inversion-recovery pulse sequence.

An overmoded rectangular cavity resonator, which focused the magnetic field on the agent at the ESR frequency of 6.45 GHz, was constructed for the actual *ex vivo* imaging. The excited resonance was a high-order mode with the linearly polarized transverse magnetic field component maximized at the bifurcated tubes containing the substance; see Fig. 1. Power was sourced from a commercial 20 W solid-state amplifier (Pascall

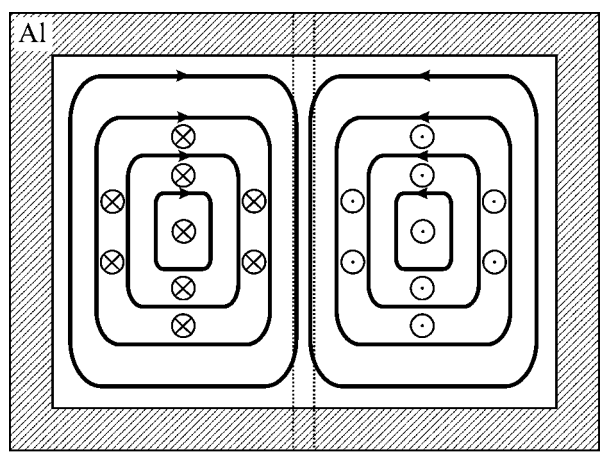

FIG. 1. The excited mode inside the aluminum cavity resonator, as seen from above. Magnetic field lines are in the plane of the page (bold lines), whereas electric field is perpendicular to the plane of the page (circles with either cross or dot, for in and out of plane, respectively). In the middle of the resonator, magnetic field reaches its maximum and electric field its minimum. The direction of $\mathbf{B}_0$ field is out of the plane of the paper. The two tubes, filled with solution, are stacked on the top of each other. Their outlines are shown as dotted lines.

Microwave, Isle of Wight, U.K.), and coupling was arranged using an electrically short loop on the one side of the resonator. The volume of the bolus that was enhanced, located in the resonant cavity, was 0.6 ml. The Q value of the resonator was approximately 100 when filled with liquid.

A simple propulsion mechanism, bearing a certain amount of resemblance to a crossbow, was integrated with the resonator. When it was triggered, two metal bars flushed out polarized fluid from the tubes and into a thin 1-mm-diameter tube going into a target, all in less than 200 ms. The trigger also contained a short-circuiting switch. This was used to synchronize the start of scan by generating a triggering event for the scanner electronics. Figure 2 shows a block diagram of the equipment used in the experiment, while Fig. 3 is a photograph of the resonator and crossbow arrangement that was used.

The apparatus was placed at the magnet isocenter and a bolus of solution containing trityl agent was irradiated in the cavity for the duration of several proton spin-lattice relaxation time constants to reach the steady-state condition. The enhancement of the proton signal was demonstrated by rapidly injecting (<200 ms) the bolus into a plastic tube going out of the resonator. The length of the tube was 0.5 m, enough for the liquid to reach the target inside the receiver coil that was also placed inside the homogeneous volume. Because the enhancement is

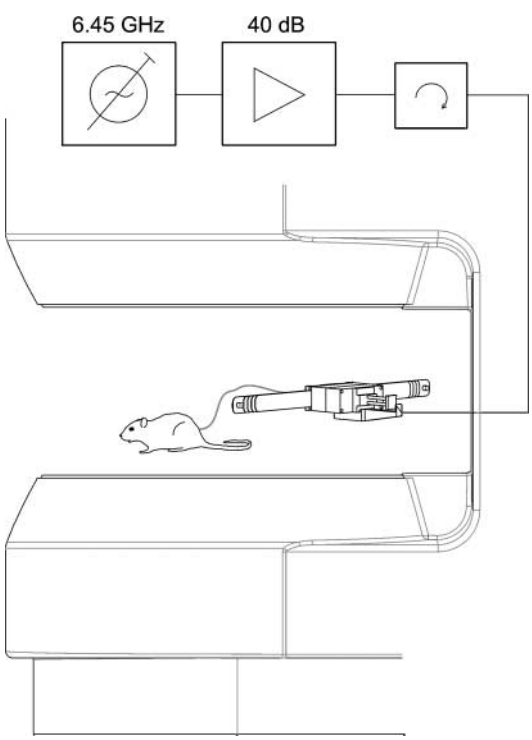

FIG. 2. Block diagram of the system used in the *ex vivo* experiment. A 6.45-GHz continuous-wave oscillator feeds the microwave amplifier, the output of which is connected to the resonator through a circulator. The circulator ensures that no power is reflected back to the amplifier. Polarized fluid is injected to the target through a plastic tube.

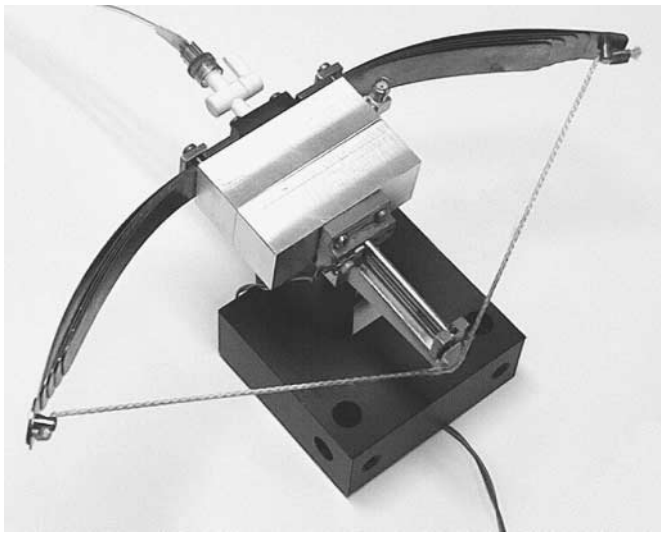

FIG. 3. Cavity resonator with propulsion mechanics.

achievable only prior to an injection, a single-shot FSE sequence (with TR/TE of $\infty/219$) was used for MR imaging in order to fully utilize the enhanced polarization. A time lag of 500 ms between the end of an injection and the start of a single-shot FSE sequence was introduced in order to avoid motion artifacts arising from the injection.

The enhancement factor was obtained by the juxtaposition of the tube with the enhanced signal with a 4.5-mm-diameter tube containing unirradiated solution. The tubes were projection-imaged, and the ratio of measured signal intensity-profiles was used to obtain the factor.

In the *ex vivo* experiment, by which the visibility of an enhanced catheter was demonstrated, the cavity was connected to a catheter lying over an anaesthetized rat. A multipurpose loop coil with an internal diameter of 210 mm was used in the experiments to detect the proton resonance signals.

RESULTS

Results for the Trityl Solution

Inversion-recovery measurements for a 5 mmol/l trityl solution at ambient temperature yielded $R_1^{II} + R_{10}^{I} = 0.67\ \mathrm{s}^{-1}$. Pure water gave R_{10}^{I} of $0.42\ \mathrm{s}^{-1}$, and hence the leakage factor could be calculated to be 0.37, indicating that the chosen concentration was still in the linear region.

The maximum obtainable enhancement ratio with completely saturated solution and without deliberately introduced delays can be calculated for the known concentration of trityl by measuring enhancement while varying irradiation power (*16*). The data are shown in Fig. 4. In this case the analysis yields a maximum enhancement of -43. This value is in good agreement with the calculated value of -40, obtained by using the above leakage factor and a coupling factor of 0.16 from the work by Ardenkjaer *et al.* (*12*), in which Eqs. [3]–[8] and the

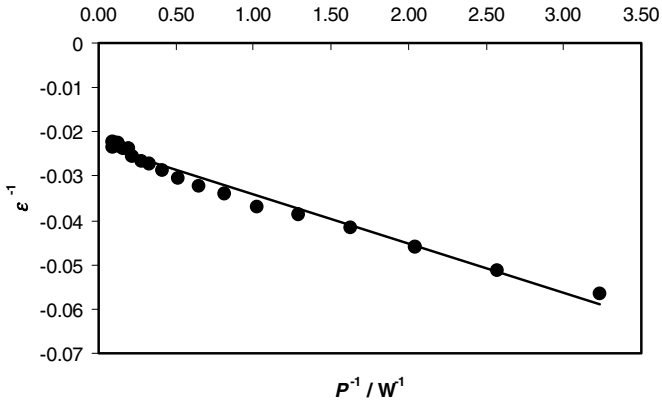

FIG. 4. Maximum enhancement. The inverse enhancement, ε^{-1}, is linearly dependent on the inverse of power, P^{-1}, and the inverse maximum enhancement can be found at the point where the fitted line ($\varepsilon^{-1} = -0.0111\,P^{-1} - 0.0232$) intercepts the y axis, cf. Ref. (*16*).

least-squares fit results for perdeuterated trityl at 23°C (presented in their Table I) are relevant. Note that the leakage factor from the fit results cannot be applied here, as it is affected by oxygen concentration. In Ref. (*12*), the experiments were performed with deoxygenated substances, whereas our test setup did not provide means for protection against air.

Ex Vivo Results

The efficiency of the *ex vivo* system was examined *in vitro* by measuring the Overhauser enhancement as a function of the power fed to the cavity. Data were recorded using the sequence noted above, with a delay Δt of 500 ms between the start of injection and the beginning of image acquisition. The highest enhancement measured from an image was −13, which was obtained with 10 W of microwave power applied at the resonance frequency. The initial enhancement at the resonator, prior to injection, can be estimated by taking into account the introduced delay and the consequent signal decay due to proton spin-lattice relaxation, i.e., the factor $\exp[-\Delta t\,(R_1^{II} + R_{10}^{I})]$. Numerically,

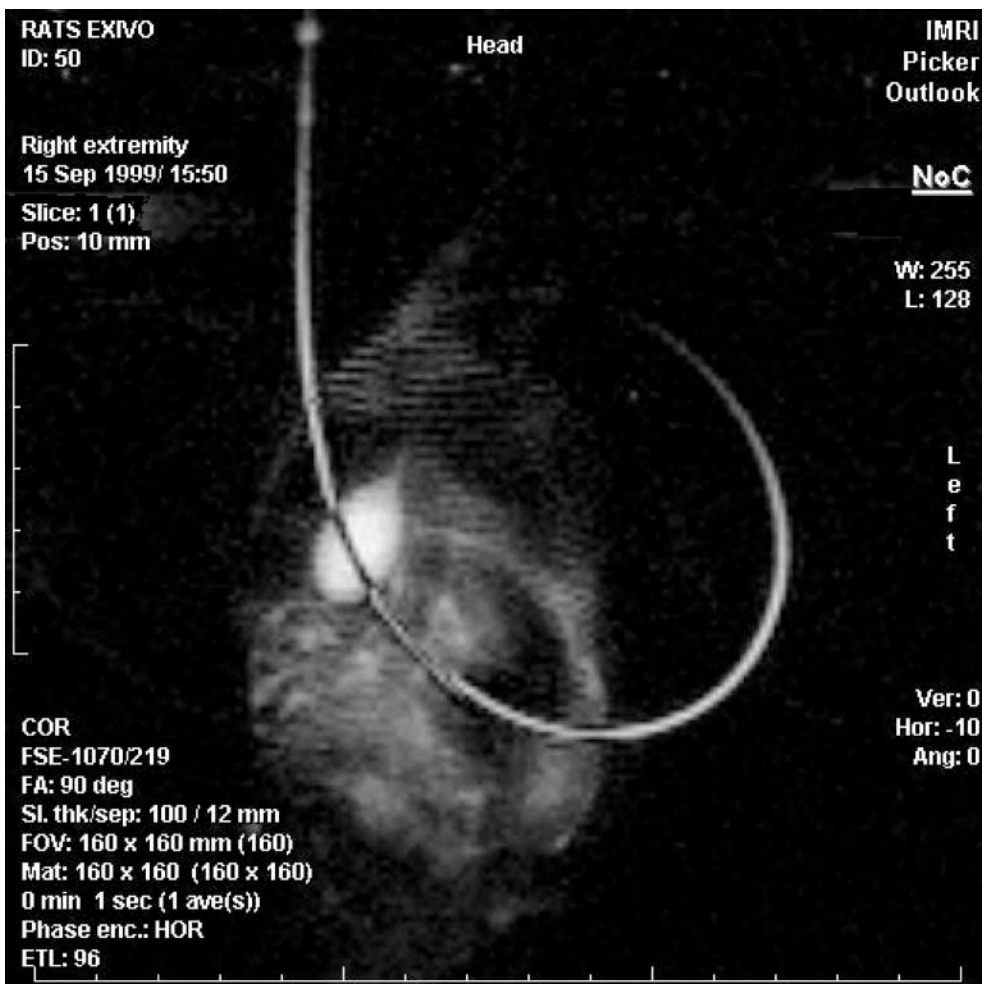

FIG. 5. Catheter filled with Overhauser-enhanced saline, placed over a rat.

the delay gives an attenuation factor of ≈0.7 for the enhancement after the injection. Leakage and coupling factors as well as the relaxation can be treated as constants, provided that physical conditions remain unchanged during the experiment—a fair assumption in this study. Maximum achievable enhancement inside the resonator can then be estimated to have been ∼20. That is, the power fed to the cavity resonator was not enough for full saturation, and the saturation factor can be estimated to have been ∼0.5.

Animal experiments were performed as described above and one result is shown in Fig. 5. This is a coronal projection image (100 mm slice thickness) of the animal in the presence of a 1-mm-diameter tube, which is of varying intensity as it wanders out of the imaging slice. The bright region in the animal is its bladder. The signal enhancement in the tube is well seen, though there were some difficulties with motion artifacts, necessitating a deliberate delay in acquiring the images as noted earlier. In view of the relatively short spin-lattice relaxation time of the solution, there was a nonnegligible loss of enhancement. One interesting effect is that where the tube overlies genuine NMR signal from the rat, signals from the two sources oppose. This is because the Overhauser enhancement is negative. The tube through which the solution was injected had a diameter of 1 mm, which is tiny compared with the bladder (∼10 mm), which emphasizes how much enhanced signal is actually obtained from the tube.

DISCUSSION

The Overhauser enhancement obtained inside the resonator was approximately half of the maximum theoretical enhancement for the solution. This is mainly due to incomplete saturation. To remedy the situation, either the irradiation power could be increased or the ESR linewidth of the trityl solution decreased. Much of the broadening can be accounted for by oxygen, which causes a substantial decrease in the relaxation times of electrons. The effect of oxygen on trityl solution has been examined in connection with Oximetric imaging by Ardenkjaer *et al.* (*12*). The broadening can be reduced by deoxygenation, which has the further advantage of increasing the leakage factor. With deoxygenated solution, an enhancement of about 65 (evaluated by setting the pure water R_{10}^I to 0.33 s^{-1}) should be possible inside the resonator. The setup in this experiment did not provide significant protection of the trityl solution from air, which prevents accurate control of the oxygen level during the course of measurements. However, the oxygenation of solution is a very slow process as compared to the loading of an injector or the saturation of solution, which means that oxygen-free packaging of solution and a more sophisticated injector should improve the situation. In order to fully utilize the enhancement, the injection time and the extra delay in avoiding motion artifacts should be minimized as well, once again necessitating a more sophisticated injector device. Overall, doubling the enhancement demonstrated in this article to 40—a rather modest goal—would reduce the striping effects visible in Fig. 5, hence enabling better detection of the catheter tip without having to rely on optimizing the sequence parameters for the relaxation time of the trityl solution. With different sequence types, the maximum usable slice thickness could be greatly increased and striping removed, but at the cost of losing the background signal. For example, using an inversion-recovery sequence, where the recovery period is adjusted to cancel out the signal from the unwanted tissue, almost all signal would come from Overhauser-enhanced liquid. The background signal could be totally eliminated by using a 90° flip angle for protons inside the resonator prior to injection. This would only excite solution and leave the background dark. With a 180° flip angle applied prior to injection, the striping would disappear even with standard sequences as the polarity of enhanced liquid would be inversed to become equal with that of tissue. The required transmitter field for protons could be produced with a dedicated coil, or, were the resonator made transparent for proton frequencies, with the standard transmitter coil. In the present study, the images were scanned with single-shot FSE. More common sequences could be utilized as well. For example, a low flip-angle gradient-echo imaging (*17*) could be used in a similar manner as in hyperpolarized helium imaging (*18, 19*); that is, only a part of the enhanced magnetization is utilized for each k-space line. EPI sequence offers also an attractive alternative for detecting the enhanced signal. Unlike in FSE, the excitation pulse flip angle can be easily changed to control the amount of the enhanced magnetization utilized for the image. Together with the fast acquisition rate of a single image by EPI, this could enable the scanning of multiple images from a single injection.

Ex vivo enhancement is an attractive concept because it avoids the need to apply microwaves *in vivo*. This is reflected in the modest requirements for additional equipment, which the Overhauser enhancement needs. A suitable resonator working at the scanner field strength of 0.23 T is much easier to construct than the equivalent, miniaturized magnet of 2–4 T needed to polarize saline to the same extent without Overhauser enhancement. The enhanced volume is close to the target and large enough for filling catheter-like structures. The handling and application of liquid are relatively straightforward; enhanced liquid can be directly injected in a variety of targets, giving a good localization effect. The ESR agent can also be introduced to a target rapidly with pressurized injection. The use of liquid also means that there is no need to introduce conductive cables or structures that are hard to sterilize into patients, which reduces the complexity and safety risks. Finally, the simplicity of the Overhauser polarization procedure itself is an advantage, as the polarizing structures can be made small and easy to handle.

In principle it would be desirable to filter the Overhauser agent out prior to delivery to the subject. This would reduce the potential problems in obtaining regulatory approval for what could be regarded as a toxic material in large quantities and, at the same time, improve the effective enhancement of saline, as the relaxivity-induced signal decay would be smaller. It would also make it possible to provide a constant influx of enhanced

liquid into the subject without any contrast agent build-up. Nevertheless, this work represents an indication that the approach is feasible, and further development could result in the elimination of many of the problems that currently impede its application in man.

REFERENCES

1. C. L. Dumoulin, S. P. Souza, and R. D. Darrow, Real-time position monitoring of invasive devices using magnetic resonance, *Magn. Reson. Med.* **29,** 411–415 (1993).
2. R. Lufkin, L. Teresi, and W. Hanafee, New needle for MR-guided aspiration cytology of the head and neck, *Am. J. Roentgenol.* **149,** 380–382 (1987).
3. N. M. deSouza, G. A. Coutts, R. K. Puni, and I. R. Young, Magnetic resonance imaging guided breast biopsy using a frameless stereotactic technique, *Clini. Radiol.* **51,** 425–428 (1996).
4. A. Glowinski, G. Adam, A. Bücker, J. Neuerburg, J. J. van Vaals, and R. W. Günther, Catheter visualization for interventional MR by actively controlled locally induced field inhomogeneities, Proceedings of the 4th Annual Meeting of International Society of Magnetic Resonance in Medicine, p. 51, 1996.
5. C. J. Bakker, R. M. Hoogeveen, J. Weber, J. J. van Vaals, M. A. Viergever, and W. P. Mali, Visualization of dedicated catheters using fast scanning techniques with potential for MR-guided vascular interventions, *Magn. Reson. Med.* **36,** 816–820 (1996).
6. C. Bos, C. J. G. Bakker, L. W. Bartels, R. van der Weide, H. J. Weinmann, and M. A. Viergever, Contrast-enhanced MR fluoroscopy: Simultaneous angiography and passive tracking of devices [abstract], *in* Proc. 9th Intl. Soc. Mag. Reson. Med., April 21–27, Glasgow, U.K., Abstract No. 2173, 2001.
7. R. Strecker, G. G. Paul, K. Scheffler, M. Hering, J. Laubenberger, and J. Hennig, Catheter tracking for MR guided selective procedures using real time projection contrast enhanced MRA: First in vivo results in a patient [abstract], *in* Proc. 9th Intl. Soc. Mag. Reson. Med., April 21–27, Glasgow, U.K., Abstract No. 2177, 2001.
8. O. Unal, F. R. Korosec, R. Frayne, C. M. Strother, and C. A. Mistretta, A rapid 2D time-resolved variable-rate *k*-space sampling MR technique for passive catheter tracking during endovascular procedures, *Magn. Reson. Med.* **40,** 356–362 (1998).
9. D. J. Lurie, J. M. S. Hutchison, L. H. Bell, I. Nicholson, D. M. Bussell, and J. R. Mallard, Field-cycled proton-electron double-resonance imaging of free radicals in large aqueous samples, *J. Magn. Reson.* **84,** 431–437 (1989).
10. R. P. Joensuu, R. E. Sepponen, A. E. Lamminen, S. E. Savolainen, and C.-G. M. Standertskjöld-Nordenstam, High-accuracy MR tracking of interventional devices: The Overhauser marker enhancement (OMEN) technique, *Magn. Reson. Med.* **40,** 914–921 (1998).
11. R. P. Joensuu, R. E. Sepponen, A. E. Lamminen, and C.-G. M. Standertskjöld-Nordenstam, A shielded Overhauser marker for MR tracking of interventional devices, *Magn. Reson. Med.* **43,** 139–145 (2000).
12. J. H. Ardenkjaer, I. Laursen, I. Leunbach, G. Ehnholm, L. G. Wistrand, J. S. Petersson, and K. Golman, EPR and DNP properties of certain novel single electron contrast agents intended for oximetric imaging. *J. Magn. Reson.* **133,** 1–12 (1998).
13. D. J. Lurie and I. Nicholson, Proton-electron double-resonance imaging of exogenous and endogenous free radicals *in vivo*, *in* "Proceedings of International School of Physics Enrico Fermi" (B. Maraviglia, Ed.), Course CXIII, pp. 485–503, Nuclear Magnetic Double Resonance, Italian Physical Society, 1993.
14. J. Trommel, Molecular motions and collisions in organic free radical solutions as studied by dynamic nuclear polarisation, Ph.D. thesis, Delft University of Technology, 1978.
15. S. Andersson, F. Radner, A. Rydbeek, R. Servin, and L.-G. Wistrand, Free radicals, US Patent 5530140, 1996.
16. H. Konijnenburg and T. Claasen-Vujčić, Overhauser imaging: Requirements, design, specification and verification, Ph.D. thesis, Delft University of Technology, 1998.
17. A. Haase, J. Frahm, D. Matthei, W. Haenicke, and K. D. Merboldt, FLASH Imaging: Rapid NMR imaging using low flip-angle pulses, *J. Magn. Reson.* **67,** 258–266 (1986).
18. H. U. Kauczor, D. Hofmann, and K. F. Kreitner, *et al.* Normal and abnormal pulmonary ventilation: Visualization by hyperpolarized He-3 MR imaging, *Radiology* **201,** 564–568 (1996).
19. J. MacFall, H. Charles, and R. Black, *et al.* Human lung air spaces: Potential for MR imaging with hyperpolarized He-3, *Radiology* **200,** 553–558 (1996).